MACROSCOPIC MODELING OF THE LINEAR-VISCOELASTIC VIBRATION BEHAVIOR OF SHORT-FIBER REINFORCED PLASTICS

Fabian Urban[a]*, Peter Middendorf[b]
[a]NVH Powertrain, Mercedes-Benz AG, Stuttgart, Germany
[b]IFB – Institute of Aircraft Design, University of Stuttgart, Stuttgart, Germany

ABSTRACT

At present, the simulation cannot satisfactorily reproduce the actual vibration behavior of short-fiber reinforced plastics. This is because the required viscoelastic material data, in particular damping, is often not available. For this purpose, a new experimental method was developed which can characterize the exact stiffness and damping of the material for a wide frequency range, taking into account environmental conditions such as temperature and humidity as well as fiber orientation. Additionally an orthotropic material model was developed, which can describe the linear-viscoelastic vibration behavior on a macroscopic level with the measured material data and a 2nd order orientation tensor from the injection molding simulation. A validation was performed on cuboid test specimens and engine mounting brackets. Results showed that the approach achieves an accuracy in calculating the resonance frequencies of <4 %. It works with thermoplastics and thermosets without an iterative reverse engineering approach but with a significant effort needed to characterize the materials.

*Corresponding author: fabian.urban@daimler.com

1. INTRODUCTION

More and more components made of short-fiber reinforced plastics (SFRP) are used in modern powertrains. They are not only of interest for the NVH (noise, vibration, harshness) improvement of conventional combustion engines, but also for high-frequency electric drives in the future. The main reason for this is the good acoustic properties due to the lower stiffness and higher damping compared to classic metallic materials. Engine mounting brackets made of SFRP are perfectly suited for this application and established in series production for several years. They transmit less structure-borne noise from the engine block to the carbody and are therefore a crucial element in the reduction of vehicle noise. In order to meet the increased customer demands regarding the acoustic value of a vehicle, a precise prediction of the vibration behavior of such components is necessary at an early stage of the development process. [1–5]

However, the simulation cannot satisfactorily predict the actual vibration behavior of fiber-reinforced plastics at present. One reason for this is that the required material data, in particular the damping, often originate from purely static tests or are completely unknown. However, dynamic, orientation- and frequency-dependent material properties are required in order

Copyright 2020. Used by the Society of the Advancement of Material and Process Engineering with permission.

to be able to reproduce the special viscoelastic properties of the SFRP. [4,6–8] For this purpose, however, there is a lack of suitable test methods to determine the exact stiffness and damping of the material for a large frequency range under consideration of environmental conditions such as temperature, humidity and fiber orientation as well as a proper material model, which can process the material data in the simulation. [9]

The present study focuses on the description of a macroscopic material model, which can process material data characterized with a new experimental method. Therefore, short-fiber reinforced thermoplastic and thermoset materials are investigated as test specimens and as an engine mounting bracket. At first, the state of the art regarding characterization and currently used methods for the description of fiber orientation and viscoelasticity is presented. The proposed approach is described beginning with the injection molding simulation followed by the orthotropic material model processing fiber orientation as well as material data. Thereafter, the material characterization is explained concluded by a method to create the material card by means of an averaged fiber orientation. Finally, the boundary conditions of the experiments and simulations carried out are described and their results are compared for validation.

2. STATE OF THE ART

2.1 Experimental Characterization

Various methods exist for the characterization of dynamic material properties. The standard ISO 6721-1 [10] generally describes methods which allow the determination of the viscoelastic parameters storage and loss modulus of plastics at different temperatures or frequencies.

The most common approach is the dynamic mechanical analysis (DMA) described in standard ISO 6721-5 [11]. In this method, a sample is excited with an oscillating force and its response behavior is measured. Force and displacement response yield stress and strain, which, together with their phase shift, allow the calculation of the storage and loss modulus. In addition to the temperature, the excitation frequency can be varied to characterize a frequency-dependent behavior. [12] The method is limited to a frequency range up to approx. 200 Hz. By using calculation approaches such as those of William-Landel-Ferry or Arrhenius, the time-temperature shift allows to conclude from a temperature-dependent to a time- and therefore frequency-dependent material behavior, thus greatly extending the usable frequency range of the material properties. [13–15] This assumption only partially applies to thermorheologically simple materials. Since plastics show phase transitions like e.g. the glass transition, they generally behave thermorheologically complex. This means that there is no clear relation between time and temperature at all and therefore no steady curve for the complex modulus by the mathematical shift approaches in the frequency domain. [1,2]

An alternative approach is the flexural resonance method. The standard ISO 6721-3 [16] describes how material properties can be derived from resonance curves of specimens. The frequency position of the resonances and the geometry of the test specimen are used to determine the storage modulus and the width of the resonance peak is used to determine the loss modulus using the 3dB-method. However, it is shown that the mounting method and contactless excitation proposed in the standard only delivers good results up to frequencies of approx. 1000 Hz. [17–19] More recent approaches to mounting, excitation and measurement for a much larger frequency range, by using e.g. a shaker and a laser vibrometer, can be found in [20–23].

2.2 Modelling of the fiber-orientation dependent material properties

There are many methods in the literature to describe the influence of short-fibers on the mechanical properties of plastics. Usually, these mathematical and physical models consist of a multi-stage homogenization method. [1]

In recent years, models based on the mean-field theory have been established. According to Böhm [24], these are approaches that describe the material in so-called Representative Volume Elements (RVE). It establishes a relationship between the outer macroscopic and the inner microscopic stresses and strains of the RVE. Using a mixing rule, the stiffness of the composite material is calculated from the material properties of the fiber and matrix material, the fiber volume fraction and a concentration tensor.

To determine the concentration tensor there are several procedures in the literature. Often the Mori-Tanaka theory [25] is applied. The idea is that the fibers are sufficiently far apart and thus decoupled from each other, so that an embedded fiber only sees the properties of the surrounding matrix. Using the fundamental Eshelby solution [26] for the mechanical relationship between fiber and matrix, the composite stiffness can be determined. One limitation, however, is the necessarily low fiber volume fraction due to the decoupling of the fibers to each other, Christensen [27] showed the applicability for a fraction of up to 30 %, Kaiser [28] also for values greater than 30 %. Possibilities for direct calculation of the engineering constants are the method according to Halpin-Tsai [29], which does not require an Eshelby solution, and the more precise method according to Tandon-Weng [30], which is based on Mori-Tanaka. Besides these 2-phase models, which only consider fiber and matrix, there are more precise approaches which allow a 3-phase consideration of fiber, matrix and interphase in between. The Reconsidered-Double-Inclusion-Model (RDI-Model) by Schöneich [31] is worth mentioning here.

However, all approaches only provide information on microstructures which fibers are all unidirectional oriented in the RVE under consideration. However, this is not the case for injection molded components. Therefore, the different fiber orientations from the injection molding simulation are divided into unidirectional, equal sections by means of 2-step homogenization, and are then weighted and superposed to a direction-dependent total stiffness. A prerequisite, however, is sufficient knowledge of the existing injection molded fiber orientation distribution in the examined object. Nowadays, this can be extracted from the injection molding simulation using process-structure coupling software that allows a transfer to the finite element (FE) mesh of the structure simulation. [1]

2.3 Modelling of the frequency-dependent viscoelastic material properties

In the literature, the description of the frequency-dependent stiffness and damping of plastics is done by mathematical formulations or approximate solutions, which however distinguish to the realistic physical behavior of the composite material. This is due to the fact that a direct characterization of the material properties is not yet possible for a large frequency range without problems. Therefore, the viscoelastic material behavior is approximated by means of substitute models. A good overview is provided by Treviso in [9]. In the following, the possibilities that are available in the common FE-programs are discussed.

If the calculation of the vibration simulation takes place in modal space, linearity must be assumed. This linearization leads to the fact that viscoelastic material models are not useable at all. Therefore, substitute models must be applied. This can for example be modal damping. It is defined as a relative part of the critical damping, is frequency-dependent but difficult to determine and can only be used isotropically. [1] Alternatively Rayleigh damping can be used. It is a linear combination of mass and stiffness matrix, i.e. a purely mathematical approach without physical considerations. It can only be defined globally for the entire model and only at exactly two frequencies. [32] However, these approaches are very simply suitable for adapting the unknown material parameters to an experiment by means of reverse engineering until the results show good agreement. This was shown for example in [2,20].

If, on the other hand, the calculation can be done by directly solving the linear system of equations, there are other possibilities. Using Prony series, the frequency-dependent material behavior can be approximated by a sum function with any number of Prony elements. For a high accuracy, however, a relatively large number is required, which in return requires a large experimental and simulative effort. [33,34] Alternatively, the viscoelastic material behavior can be transferred directly to the FE-program as storage and loss modulus in a Jacobian matrix. [32]

3. PROPOSED APPROACH

3.1 Overview

The existing methods for the vibration simulation of SFRP have been successfully using microscopic approaches. A major problem is the lack of a characterization method to measure viscoelastic material properties for a wide frequency range. The data is still mathematically extrapolated from low frequencies or determined by means of a reverse engineering approach and not directly measured.

The proposed approach therefore follows a different path. By means of a new more advanced experimental method, SFRP can be characterized in a wide frequency range as a function of temperature, humidity and fiber orientation. The viscoelastic material data can be used directly in the FE-simulation by using a macroscopic material model. Figure 1 gives an overview of the approach.

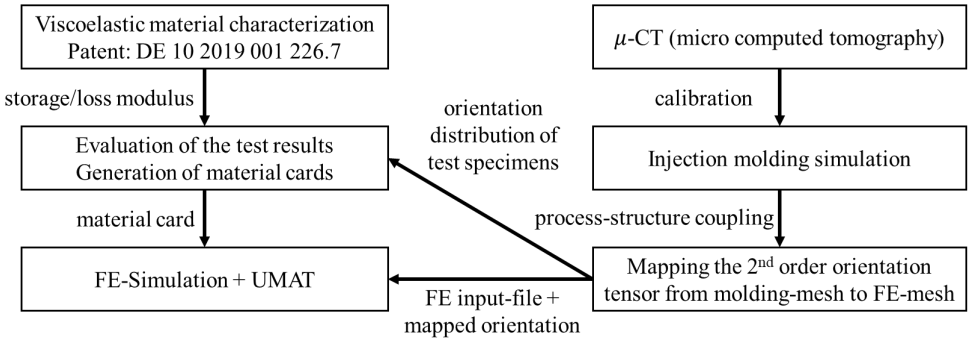


Figure 1. Overview of the proposed approach

The injection molding simulation is calibrated with the micro computer tomography (μ-CT) and the fiber orientation is then mapped onto the FE-mesh of the structure simulation. The flexural

vibration of the test specimens is measured and analyzed. Storage and loss modulus are determined for every resonance frequency. Together with the averaged fiber orientation for every measured specimen the frequency and orientation dependent material card is calculated. It is then read and processed by the FE user-material (UMAT). For every calculated frequency step the implemented material model fills an own complex orthotropic stiffness matrix for every element of the structure simulation FE-mesh.

3.2 Fiber orientation

During the injection molding process a characteristic cross-sectional profile of the injection molded component is observed. It can be approximated using a 3-layer model. In the outer layers, the shear effects at the borders of the injection mold cause the fibers to align in the direction of flow. In the middle of the flow path, an alignment of the fibers transverse to the flow direction can be observed. The thickness of the middle layer depends essentially on the velocity profile of the flow and thus on the viscous properties of the plastic used and its process parameters. [1]

The common tools of injection molding simulation use variations of the Folgar-Tucker model and its extension the Reduced-Strain-Closure model. Advani and Tucker [35] developed the possibility to describe the orientation distribution in the form of a local orientation tensor of 2nd or 4th order. For the elastic consideration, the 2nd order orientation tensor is sufficient. [1,36] The calculation of especially thermosets is still problematic. The curing reaction must be considered and characteristic values are hardly available. Therefore, the fiber orientation distribution of the injection molding simulation should be validated with a µ-CT analysis and calibrated if necessary.

Since the FE-mesh of process and structure simulation are completely different, the calculated fiber orientation distributions, i.e. the orientation tensor, must be transferred from the finer injection molding mesh to the coarser structure simulation mesh using a process-structure coupling software. For this purpose, the "Nearest-Neighbor method" is used to enable a corresponding assignment. The orientation tensor then provides information about the orientation in the local element in the form of a local eigenvector pointing in the main direction with the most fibers. The eigenvalues describe the percentage of fibers in the main and the other directions of the Cartesian coordinate system, which differs from element to element. [1]

3.3 Material model

The aim is to use the viscoelastic material properties from the experiment directly and macroscopically. To assign an orthotropic stiffness matrix to each FE-element, the material data is taken directly from a large, universally valid material card using an angle-dependent description. The 2nd order orientation tensor from the injection molding simulation provides eigenvectors and eigenvalues that locally describe the main direction of the fibers and their percentage in the respective directions. Therefore, a material model linking eigenvalues and angle-dependence is required.

First, the different coordinate systems shown in Figure 2 must be explained. In the global FE-coordinate system (x,y,z) each element receives a local orientation coordinate system consisting of three eigenvectors (1,2,3) defined in the x,y,z-system. The 1-vector points in the direction in which the largest percentage of fibers in the element is oriented. The eigenvalues (EV_1,EV_2,EV_3) indicate the percentage of fiber in the respective directions of the 1,2,3-system and have the sum

of 1. Now a homogenization takes place by forming the resulting vector $\vec{p}_{hom}$ in the 1,2,3-system with the three eigenvalues in order to consider fiber influences of all directions in the local element. The relative deviation of the homogenized vector to the local 1,2,3-system thus contains the information about the stiffness of the element.

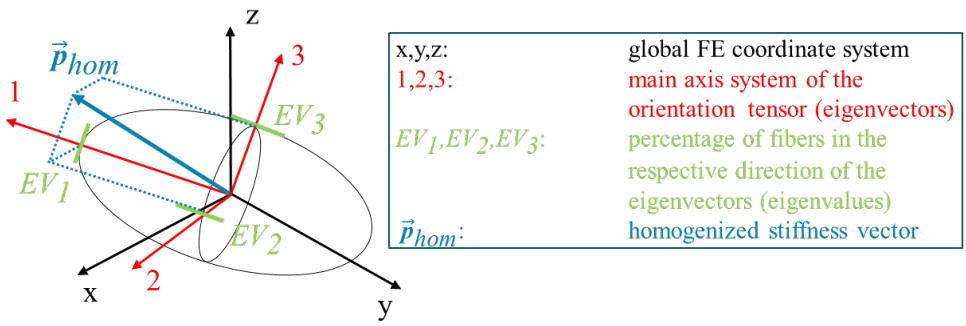


Figure 2. Coordinate systems of a local macroscopic FE-element

Figure 3 shows how to conclude an angle-dependent local element description from the deviation of $\vec{p}_{hom}$ to the 1,2,3-system. Assuming that the eigenvalue 1 is equal to 1, the other eigenvalues have to be equal to 0. In this case, the homogenized vector points in the direction of the 1-axis and all fibers in the element are oriented in this direction. Thus, the element would have an ideal relative angle of 0°-stiffness with all fibers in this direction, which corresponds to the ideal high stiffness of the 1-axis. If, on the other hand, the eigenvalues 2 or 3 are equal to 1, the homogenized vector would point in the corresponding direction. The stiffness of the local element relative to the 1-direction would thus have an ideal relative angle 90°-stiffness with all fibers in those directions, which therefore corresponds to the ideal low stiffness of the 2- and 3-axis. The real homogenized vector moves in between. By means of projection in the 12- and 13-plane, a relative deviation angle ϕ and θ from the 1-axis is obtained, which varies between 0° and 90°.

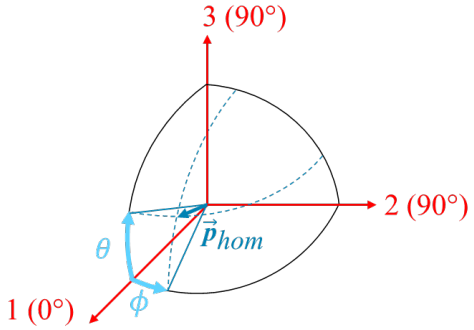


Figure 3. Local orientation projection into the 12- and 13-plane

Therefore, the local stiffness in the 1,2,3-coordinate system in the 1-direction results from the relative deviation of ϕ and θ from the 1-axis with the storage modulus $E'(\phi)$ and $E'(\theta)$ taken from the angle-dependent material card to

$$E_1' = \frac{E'(\phi) \cdot EV_2 + E'(\theta) \cdot EV_3}{EV_2 + EV_3}. \quad (1)$$

The eigenvalues are used to allow a relative weighting of the fiber quantity for the respective direction. To calculate the stiffness in the 2- and 3-directions, the quadrants have to be switched and the homogenized vector has to be completed to a Cartesian coordinate system. Its projected angular deviation from the 2-axis and to the 3-axis results in the respective stiffness

$$E_2' = \frac{E'(90° - \phi) \cdot EV_1 + E'(90°) \cdot EV_3}{EV_1 + EV_3}, \tag{2}$$

$$E_3' = \frac{E'(90°) \cdot EV_2 + E'(90° - \theta) \cdot EV_1}{EV_2 + EV_1}. \tag{3}$$

Equations (1-3) can be used in the same way for the loss modulus. Thus, the complex orthotropic stiffness matrix in Figure 4 can now be filled locally for the considered element. Finally, it must be transformed back into the global x,y,z-coordinate system with the coordinates of the eigenvectors in order to perform the FE-calculation.

$$\begin{bmatrix}\sigma_{11}\\ \sigma_{22}\\ \sigma_{33}\\ \sigma_{12}\\ \sigma_{13}\\ \sigma_{23}\end{bmatrix} = \begin{pmatrix} \frac{1-\nu_{23}\nu_{32}}{D}E_1^* & \frac{\nu_{13}\nu_{32}+\nu_{12}}{D}E_2^* & \frac{\nu_{12}\nu_{23}+\nu_{13}}{D}E_3^* & 0 & 0 & 0 \\ & \frac{1-\nu_{13}\nu_{31}}{D}E_2^* & \frac{\nu_{21}\nu_{13}+\nu_{23}}{D}E_3^* & 0 & 0 & 0 \\ & & \frac{1-\nu_{12}\nu_{21}}{D}E_3^* & 0 & 0 & 0 \\ & & & G_{12}^* & 0 & 0 \\ & sym & & 0 & G_{13}^* & 0 \\ & & & 0 & 0 & G_{23}^* \end{pmatrix} \begin{bmatrix}\epsilon_{11}\\ \epsilon_{22}\\ \epsilon_{33}\\ 2\epsilon_{12}\\ 2\epsilon_{13}\\ 2\epsilon_{23}\end{bmatrix}$$

$$D = 1 - \nu_{12}\nu_{21} - \nu_{13}\nu_{31} - \nu_{23}\nu_{32} - 2\nu_{21}\nu_{32}\nu_{13}$$

$$\nu_{21} = \frac{E_2^*}{E_1^*}\nu_{12}, \qquad \nu_{31} = \frac{E_3^*}{E_1^*}\nu_{13}, \qquad \nu_{32} = \frac{E_3^*}{E_2^*}\nu_{23}$$

$$\text{Approximation: } G_{jk}^* = \frac{E_j^* E_k^*}{E_j^* + 2\nu_{jk}E_j^* + E_k^*}; j, k := \{1,2,3\}$$

Figure 4. Complex orthotropic stiffness matrix [32,37]

3.4 Experimental Characterization

At first, cuboid test specimens are cut out of a flat injection molded plate in different orientations relative to the flow direction, see Figure 5.

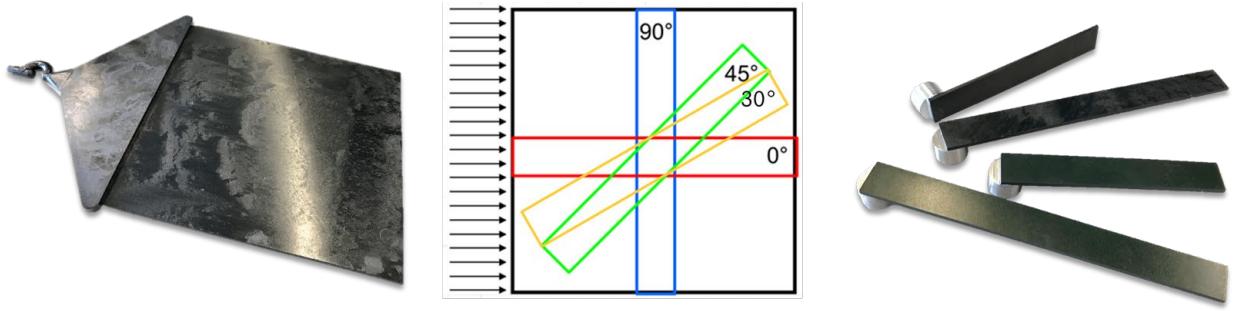


Figure 5. Preparation of test specimens (left to right: injection molded plate, cutting orientations, test specimens with specimen-adapter)

The experimental characterization method of the viscoelastic material properties originates from the self-developed patent [38] which is based on the flexural resonance method in Chapter 2.1. The functional principle and the real mounting structure is shown in Figure 6.

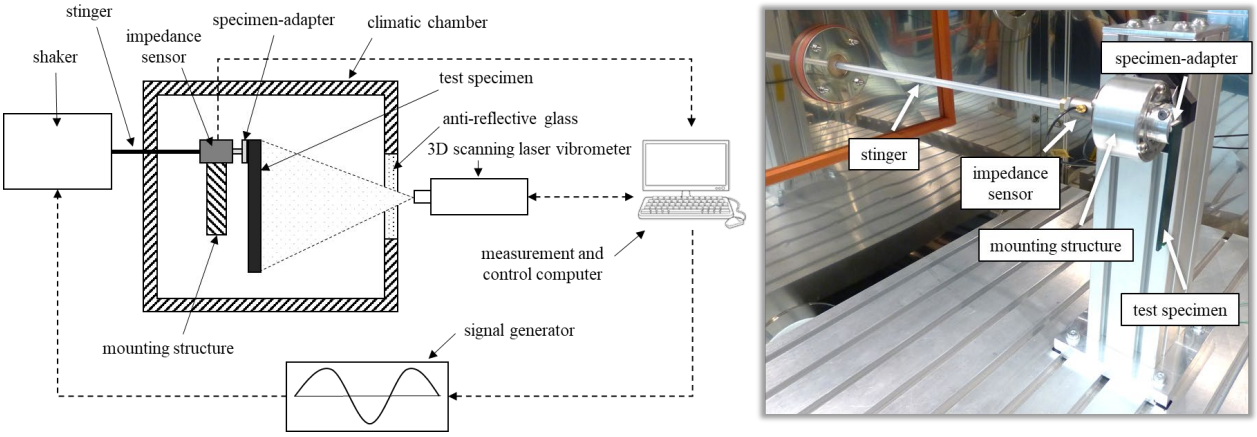


Figure 6. left: principal test setup, right: mounted specimen in climatic chamber

The properties of plastics are very sensitive to even small changes in temperature and humidity. A climatic chamber allows constant ambient conditions during the tests. A possible operating range of -30 °C to 220 °C requires that the sensitive equipment is located outside the climatic chamber. The sensor measuring the excitation, as well as the mounting structure must be located inside the climatic chamber and therefore be temperature and humidity resistant.

The specimens are mounted in a fixed-free suspension inside the climatic chamber and excited with a sinusoidal sweep by a shaker. The stinger transmits the excitation into the chamber and through the impedance sensor measuring force and acceleration into the mounted specimen. Using a laser vibrometer, the flexural vibration response is measured at the free end of the specimen. Dividing the resulting acceleration a with the excitation force F yields the accelerance frequency response function (FRF) a/F $[\frac{\mathrm{m}}{\mathrm{s}^2}/\,\mathrm{N}]$. Since linear-viscoelastic material behavior is assumed, there is a linear relationship between the excitation force as energy introduced into the system and the resulting acceleration of the test specimen. By using the force normalization, the measured and evaluated FRF does not change despite a fluctuation of the excitation force in the test. The FRF is therefore comparable and reproducible.

By varying the excitation frequency, any number of resonance orders up to a frequency of 10 kHz can be evaluated from the FRF. From the i-th resonance frequency f_i of the flexural vibration, together with the length l and thickness h of the test specimen, the density ρ of the material and the fixed-free suspension condition k_i, the storage modulus E' in each resonance frequency can be determined by means of a transformed Bernoulli bar theory according to [16] with

$$E'_f = \frac{48\pi^2\rho l^4}{h^2}\frac{f_i^2}{{k_i}^4};\ k_i = (i-0{,}5)^2\pi^2. \tag{4}$$

The loss factor $tan(\delta)$ is determined with the 3dB-method from the i-th resonance frequency width Δf_i at which the amplitude of the FRF resonance peak has fallen on both sides by 3 dB and the resonance frequency f_i with

$$tan(\delta)_f = \frac{\Delta f_i}{f_i}. \tag{5}$$

The loss modulus E'' can now be calculated using (4) and (5) with

$$E''_f = E'_f \cdot tan(\delta)_f. \tag{6}$$

Storage and loss modulus can only be determined in the resonance frequencies of the test specimens. Depending on stiffness, geometry and density, this can include more than a dozen resonances up to a frequency of 10 kHz. Viscoelastic material data can be calculated for each of the resonance frequencies. By interpolating between these discrete data points, a frequency-dependent curve can be determined. However, the sample has to show a pure flexural vibration without a superimposed, e.g. torsional mode. In addition, the test setup should not show any resonance behavior itself, the laser has to measure a good quality signal on the sample and the energy introduced by the shaker must be sufficiently high even at high frequencies.

Although the test setup can be used universally for non-reinforced plastics or other classes of materials, the focus is on SFRP. For an orientation dependence, test specimens are cut out in an orientation relative to the flow direction from an injection molded plate. However, experience shows only 75 % of the fibers are oriented in the flow direction, the remaining fibers are oriented in the transverse and thickness direction. Therefore, fully oriented test specimens are not available for injection molding but rather a mixed composition varying with the cutting direction of the specimens.

3.5 Generating a material card

In order to be able to fill equations (1-3) with angle-dependent storage and loss modulus, a comprehensive material card is required. The characterization is carried out using specimens cut-out from injection molded plates. However, the cutting direction has nothing to do with the fiber orientation angles required in the material model. Therefore, a method has to be found to conclude from a cutting orientation to a fiber orientation, which can be used to fill the material card with the measured data.

First, the evaluation procedure and the generation of material cards must be explained. Since viscoelastic material data has to be calculated directly in the FE-simulation, an update of the stiffness matrix can take place for every frequency step. Thus, for each a material card with angle-dependent storage and loss modulus is needed. The procedure is shown in Figure 7. The measured FRF is evaluated in its resonance frequencies. The material data determined on several test specimens of the same cutting orientation are averaged and interpolated in the frequency domain. Afterwards a swap of the order of values takes place and for each interpolated frequency, an angle-dependent function is generated by interpolation between the measured orientations. These data are stored as discrete points in a material card for a given temperature and humidity, so that the FE-simulation can search for the required material properties.

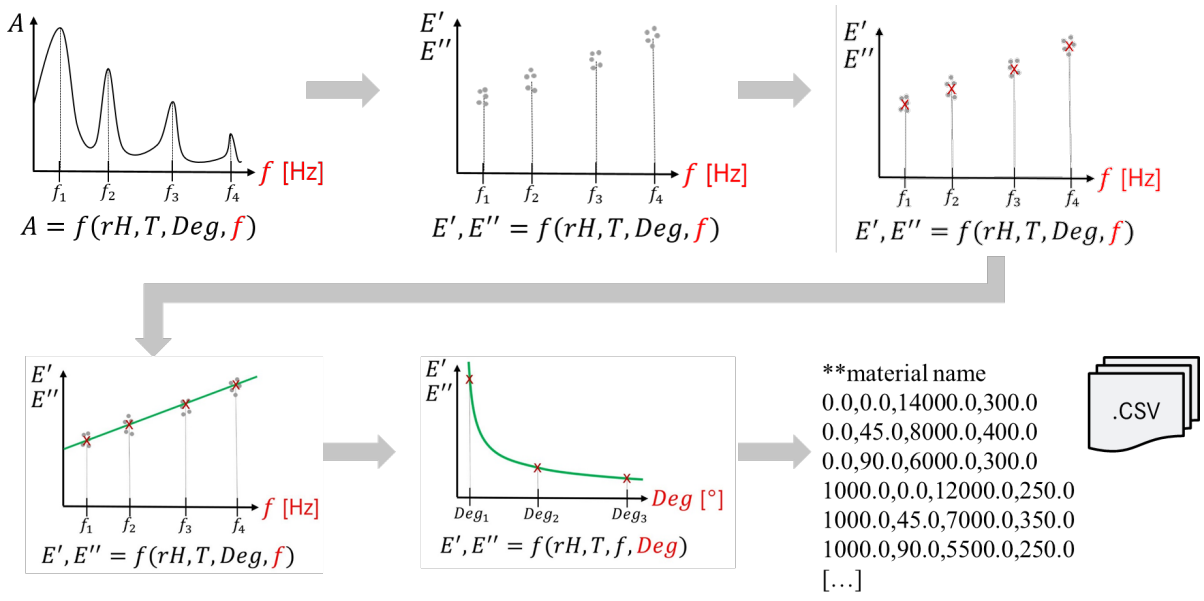


Figure 7. Generation of a material card from a FRF

The measured specimens have an averaged stiffness of all fiber orientation distributions that occur in them. It is assumed that the averaged deviation of all macroscopic elements of a test specimen corresponds to the stiffness value measured with it. In order to determine the correct averaged orientation angle, the material model must now be calculated backwards. To do this, the averaged absolute orientation direction in the global coordinate system is determined for each cut-out specimen using the injection molding simulation of the plate from which the specimens are prepared. These directions are shown as arrows in Figure 8 and differ from each other. The angular deviation from their respective cutting orientation yields the averaged fiber orientation angle. It corresponds to the measured specimen stiffness. This is shown in Figure 8 for example for the 45°-specimen. The determined averaged angles can now be used for inter- and extrapolation of the material card in the angle domain and thus in the FE-calculation.

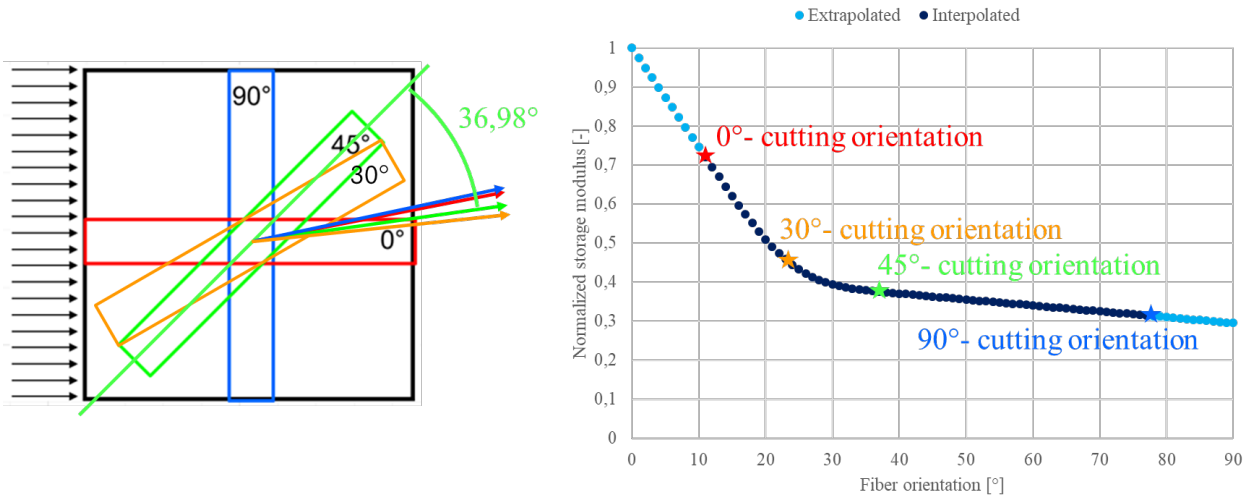


Figure 8. Conclusion from a cutting orientation to an averaged fiber orientation

The injection molding simulation is deliberately used to determine the average fiber orientation of the test specimens, rather than the more precise information from a CT analysis. This is because only a few small sections of the specimens can be examined in the µ-CT and not their entirety, which can lead to a significant error. In addition, all further calculations are carried out with the same injection molding model that has already been calibrated with a CT analysis.

4. RESULTS

4.1 Experimentation

The tests are carried out with two different injection moldable materials. On the one hand, a polyamide 6.6 with 50 weight-% short glass fibers (PA66-GF50) is used as a representative of the thermoplastics, on the other hand, a phenolic resin with 55 weight-% short glass fibers (PF-GF55) is used as a representative of the thermoset plastics in order to show a universal applicability of the approach. Cuboid test specimens are prepared from injection molded plates. The thermoplastic specimens are prepared in the directions 0°, 30°, 45°and 90° with the lengths 180 mm and 140 mm as well as a width of 15 mm and a thickness of 2 mm from a 180x180x2 mm plate. The thermoset samples are prepared in the directions 0°, 45° and 90° with the lengths of 170 mm and 130 mm as well as a width of 15 mm and a thickness of 2 mm from a 171,5x171,5x2 mm plate. For each orientation and length, three specimens are prepared, each of which is cut out at the identical positions from the injection-molded plate. They are then at an end on an area of 5x15 mm attached to a specimen-adapter with a two-component epoxy resin adhesive and cured. Afterwards, the real geometry, i.e. the freely oscillating length as well as the thickness and the density, are measured for each sample in order to determine the storage modulus free of geometric or material fluctuations.

A Weiss-Technik ClimeEvent C/600/40/3 climatic test chamber and a Polytec PSV-500-3D-Xtra scanning laser vibrometer are used for the experiments. The samples are now dried or wet conditioned for the respective test according to the material manufacturer's specifications and left in a constant climatic environment for some time before the tests. Temperature and humidity investigated range between 0 °C and 130 °C for 0 %RH (relative humidity) and between 0 °C and 50 °C for 50 %RH. Engine mounting brackets freely suspended in the climatic chamber are also examined, which are conditioned and stored according to the same specifications. The Polytec PSV Software is used for the analysis of the laser measurements, the calculation of the material card is performed by a VBA-Script (Visual Basic for Applications).

For calibration and validation of the injection molding simulation, µ-CT investigations are performed on samples with the size 5x5x2 mm. They are taken from the injection molded plate so that each specimen is covered by three different positions along its length.

4.2 Simulation

The injection molding simulation is performed with CADMOULD, the mapping with CONVERSE. Hereby up to ten different fiber orientation layers over the thickness of the examined object can be transferred to a structure simulation mesh. The meshing is carried out for the test specimens with ABAQUS and for the engine mounting brackets with SIMLAB. The simulation is performed as a direct-solution steady state dynamic analysis with a UMAT programmed in FORTRAN. The UMAT reads in the material card and the 2nd order orientation tensor, sorts them

and stores them for the simulation. In the material card, the data set for storage and loss modulus closest to the calculated frequency step is then searched for and the required data is interpolated for each element from the angular distribution to fill the complex stiffness matrix. Then the eigenvectors for each element are passed to ABAQUS to rotate the matrix into the global coordinate system.

The specimen is meshed with the easily stretchable C3D20 elements, see Figure 9. This is because it is very important to use all ten fiber orientation layers, in order to correctly reproduce the stiffness of the overall composite without causing too much computing time. The engine mounting bracket is meshed with Tet elements, because the geometry is much more complex and thus a sufficient number of layers can be transferred from the injection molding simulation.

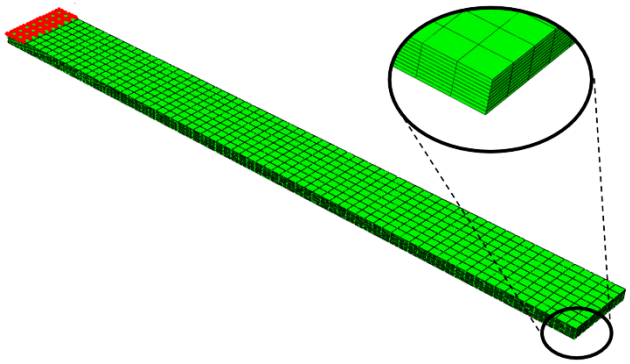


Figure 9. FE-mesh of the test specimen

Excitation and mounting conditions of the test specimen are modelled according to the test setup. Its movement is blocked at one end on an area of 5x15 mm in all spatial directions except in the thickness direction, where it is excited for all frequencies with constant acceleration of 1 mm/s². The FRF is calculated in a comparable way by evaluating the acceleration at the same point on the specimen as in the experiment and normalizing it with the excitation force. Furthermore, linear-viscoelastic material behavior, a constant fiber orientation in each element, constant material properties across a FE-element for all integration points and equal treatment of thermoplastic and thermoset are assumed. Additionally, the orthotropic shear modulus in Figure 4 can be calculated as an approximate function of Young's modulus and Poisson's ratio. Due to the limited availability of data and the little influence on the results, the Poisson's ratio is assumed directional but frequency independent and taken from a material database.

4.3 Results

First, the comparison of µ-CT and injection molding simulation takes place. Figure 10 shows the orientation tensor over the normalized thickness of the specimen at an exemplary location near the sprue. The solid line is taken from the CT measurement. Green represents the inflow, blue the crossflow and yellow the thickness direction. The crosses show the positions across the thickness at which data from the injection molding simulation is extracted, in total at a maximum of 10 possible locations.

The thermoplastic shows a narrow middle layer with a rapidly shifting orientation towards this area. Over the remaining thickness, the orientation is somewhat constant. The line from the CT

examination is approximated very well, but the exact mid-layer cannot be analyzed due to the algorithm of the injection molding simulation. The thermoset, on the other hand, drops continuously towards the middle and therefore does not have a clearly shaped middle layer but rather a continuous transition of the orientation distribution. The CT measurement is approximated well by the injection molding simulation inflow, crossflow is slightly overestimated and the thickness direction is slightly underestimated.

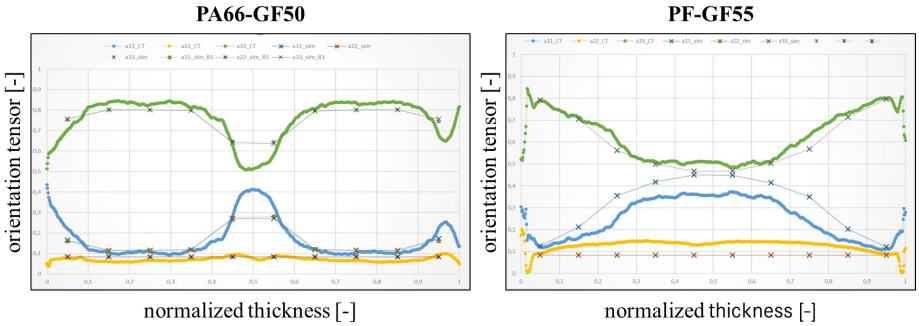


Figure 10. Results of the measured and simulated orientation tensor (green/blue/yellow line: inflow/crossflow/thickness direction from the µ-CT analysis, crosses with lines: corresponding data from the injection molding simulation)

In the following, the comparison between experiment and simulation of the test specimens used to create the material card is carried out. Figure 11 shows the thermoplastic PA66-GF50. The comparison illustrates the double logarithmic FRF exemplary for 23 °C and 0 %RH for the orientations 0°, 45° and 90° and a specimen length of 140 mm, in red the simulation and in blue the experiment. Both the resonance frequency positions and the amplitude peaks match very good at almost all resonances. Deviations in the amplitude can result from superposition of other modes of vibration in the experiment. The comparison shows that the maximum deviation of the resonance frequencies is <3 % and the amplitude peak <10 % for the 0°-specimen. The other orientations show an even better agreement.

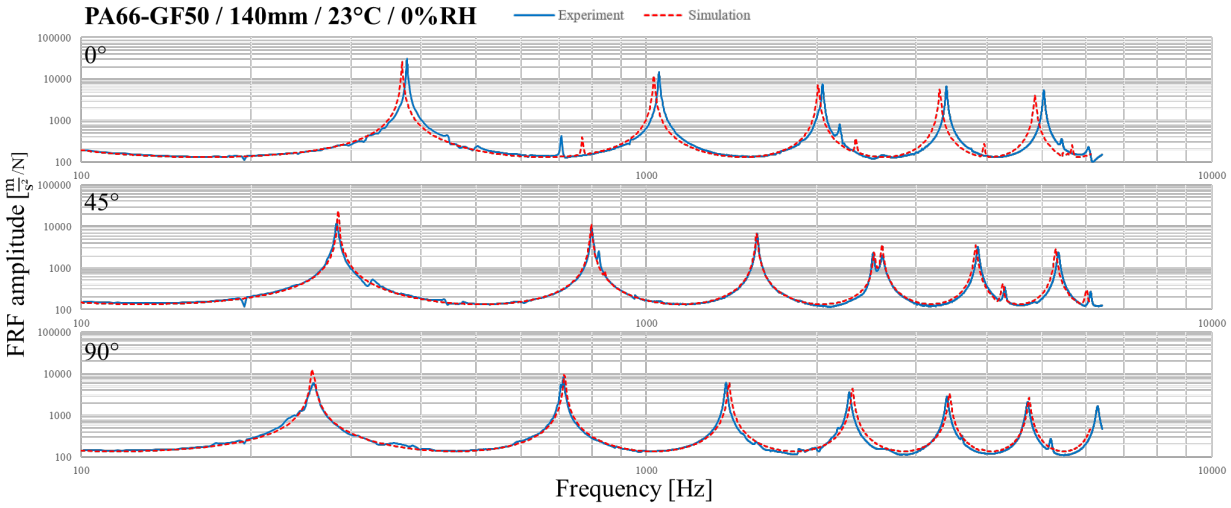


Figure 11. Results experiment/simulation of thermoplastic PA66-GF50

The comparison of the thermoset material is analogous to the thermoplastic but with a 170 mm specimen and shown in Figure 12. Resonance frequency positions and amplitude peaks fit very well. Like with the thermoplastic the 45° sample has a good accuracy. The largest deviation of the resonance frequencies is <4 % and the amplitude peak is <15 % for the 90°-specimen.

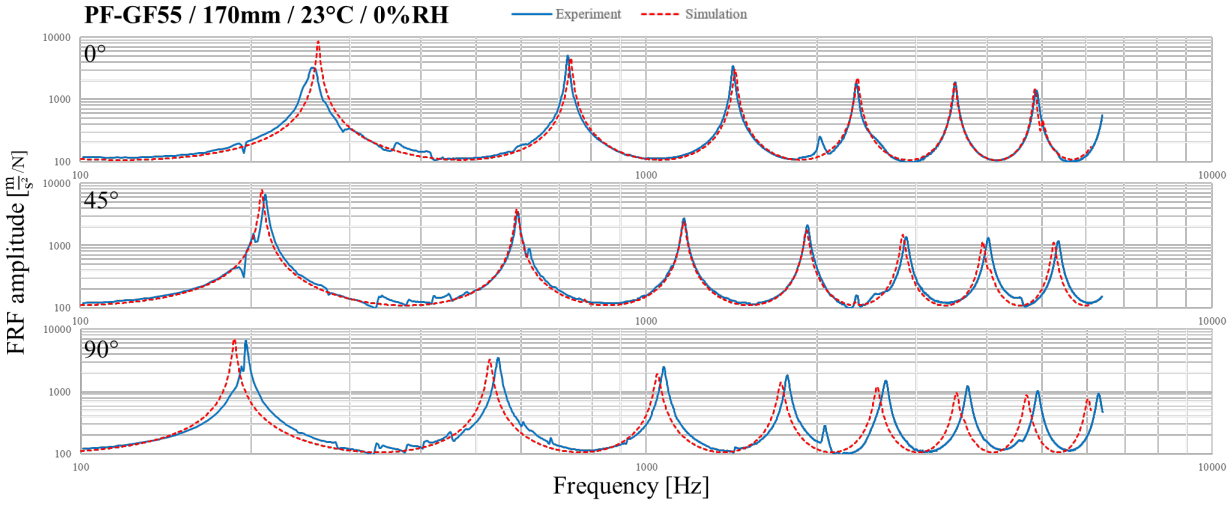


Figure 12. Results experiment/simulation of thermoset PF-GF55

Finally, an engine mounting bracket made out of PA66-GF50 is simulated. This component is quite complex and comprehensive in terms of geometry and fiber distribution. Particular difficulty is due to the correct mounting in the experiment and the modelling in the simulation. The results in Figure 13 are very significant. The deviation of the resonance frequencies from simulation to experiment is <3 %.

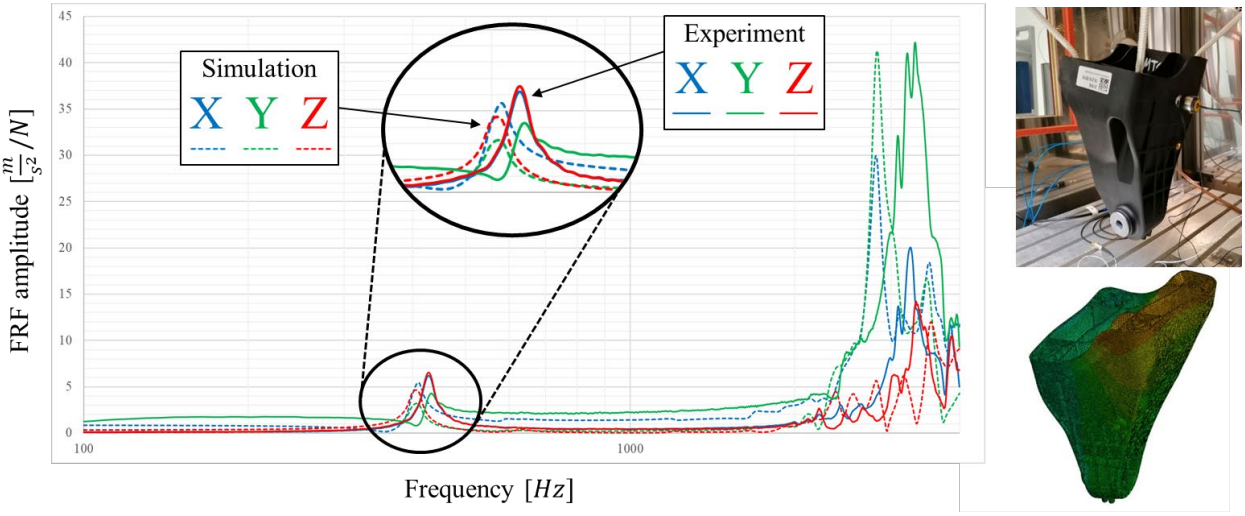


Figure 13. Results experiment/simulation of an engine mounting bracket made of PA66-GF50

5. CONCLUSIONS

A novel approach for vibration calculation of SFRP was presented. It was shown that macroscopic composite data can be used to model the linear-viscoelastic material behavior. The results show a good agreement with the experiment without mathematical approximation solutions or iterative reverse engineering approaches.

It should be noted that the results of the test specimens do not necessarily have to agree, as they serve as a basis for the material card. Rather, it was shown that the approach succeeds in creating the angle-dependent function of the storage and loss modulus and reassembling it again to create an overall composite of different orientation distributions and thus direction-dependent stiffness. Especially the orientation of 45° is to be emphasized, since the shear modulus and its approximate solution is particularly influential here and the results have shown a good agreement. Furthermore, a 2nd order orientation tensor was sufficient for this approach, as well as the maximum of 10 layers from the injection molding simulation to correctly reproduce the overall composite of the material. Finally, it was shown that the approach works well not only for thermoplastics but also for thermosets. The latter had been difficult to model so far, because the material had to be understood on a microscopic level. By means of the new approach, this is no longer necessary.

The disadvantage, however, was that the effort required to create the material card as well as the resource consumption of the simulation is relatively high. Since the material card can be used universally, the method is suitable for areas where the same material is used for different components.

6. REFERENCES

[1] Stommel, M., Stojek, M., Korte, W. *FEM zur Berechnung von Kunststoff- und Elastomerbauteilen*, München: Hanser, 2nd ed., 2018. DOI: 10.3139/9783446452831.

[2] Kremer, H. *Materialdatenermittlung thermoplastischer Kunststoffe für Körperschallsimulationen auf Basis von Reverse Engineering*. PhD thesis, Aachen: Mainz, 2014.

[3] Raschke, K., Korte, W. "Faserverstärkte Motorbauteile besser berechnen." *Kunststoffe* 109 (2019): 184–189.

[4] Laak, M. op de, Hauth, M. "Noch schneller zur Zylinderkopfhaube." *Kunststoffe* 94 (2004): 126–130.

[5] Michaeli, W., Hopmann, C., Kremer, H. "Materialdatenermittlung für Akustiksimulationen mittels Reverse Engineering: Akustisches Verhalten von Kunststoffen." *Kunststoffe* 102 (2012): 5–7.

[6] Giersbeck, M., Hornberger, K., Kech, A. "Virtuelle Bauteilentwicklung." *Kunststoffe* 101 (2011): 50–53.

[7] Hopmann, C., Michaeli, W., Kremer, H. "Frequenzabhängiges Verhalten von Kunststoffen." *Kunststoffe* 102 (2012): 64–66.

[8] Pischinger, S., Michaeli, W., Joerres, M., Steffens, C., Atzler, M., Arping, T. "Verfahren zur akustischen Simulation von Kunststoffbauteilen." *MTZ - Motortechnische Zeitschrift* 70 (2009): 692–701. DOI: 10.1007/BF03225522.

[9] Treviso, A., van Genechten, B., Mundo, D., Tournour, M. "Damping in composite materials: Properties and models." *Composites Part B: Engineering* 78 (2015): 144–152. DOI: 10.1016/j.compositesb.2015.03.081.

[10] ISO 6721-1, 2019. "Plastics — Determination of dynamic mechanical properties — Part 1: General principles" International Organization for Standardization, Geneva, 2019, https://www.iso.org/obp/ui/#iso:std:iso:6721:-1:ed-4:v1:en.
[11] ISO 6721-5, 2019. "Plastics — Determination of dynamic mechanical properties — Part 5: Flexural vibration — Non-resonance method" International Organization for Standardization, Geneva, 2019, https://www.iso.org/obp/ui/#iso:std:iso:6721:-5:ed-2:v1:en.
[12] Menard, K. P. *Dynamic Mechanical Analysis: A Practical Introduction*, Hoboken: Taylor & Francis, 2nd ed., 2008. DOI: 10.1201/9781420053135.
[13] Menges, G., Haberstroh, E., Michaeli, W., Schmachtenberg, E. *Menges Werkstoffkunde Kunststoffe*, München: Hanser, 6th ed., 2011. DOI: 10.3139/9783446443532.
[14] Keuerleber, M. *Bestimmung des Elastizitätsmoduls von Kunststoffen bei hohen Dehnraten am Beispiel von PP*. PhD thesis, Stuttgart, 2006.
[15] Arping, T. W. *Werkstoffgerechte Charakterisierung und Modellierung des akustischen Verhaltens thermoplastischer Kunststoffe für Körperschallsimulationen*. PhD thesis, Aachen: Mainz, 2010.
[16] ISO 6721-3, 1994. "Plastics — Determination of dynamic mechanical properties — Part 3: Flexural vibration — Resonance-curve method" International Organization for Standardization, Geneva, 1994, https://www.iso.org/obp/ui/#iso:std:iso:6721:-3:ed-1:v1:en.
[17] Berthelot, J.-M., Assarar, M., Sefrani, Y., Mahi, A. E. "Damping analysis of composite materials and structures." *Composite Structures* 85 (2008): 189–204. DOI: 10.1016/j.compstruct.2007.10.024.
[18] Bonfiglio, P., Pompoli, F. "Determination of the dynamic complex modulus of viscoelastic materials using a time domain approach." *Polymer Testing* 48 (2015): 89–96. DOI: 10.1016/j.polymertesting.2015.09.016.
[19] Crane, R. M., Gillespie, J. W. "Characterization of the vibration damping loss factor of glass and graphite fiber composites." *Composites Science and Technology* 40 (1991): 355–375. DOI: 10.1016/0266-3538(91)90030-S.
[20] Ilg, J. *Bestimmung, Verifikation und Anwendung frequenzabhängiger mechanischer Materialkennwerte*. PhD thesis, München: Dr. Hut, 2015.
[21] Belder, K. de, Pintelon, R., Demol, C., Roose, P. "Estimation of the equivalent complex modulus of laminated glass beams and its application to sound transmission loss prediction." *Mechanical Systems and Signal Processing* 24 (2010): 809–822. DOI: 10.1016/j.ymssp.2009.11.001.
[22] Cortés, F., Elejabarrieta, M. J. "Viscoelastic materials characterisation using the seismic response." *Materials & Design* 28 (2007): 2054–2062. DOI: 10.1016/j.matdes.2006.05.032.
[23] El-Hafidi, A., Gning, P. B., Piezel, B., Belaïd, M., Fontaine, S. "Determination of dynamic properties of flax fibres reinforced laminate using vibration measurements." *Polymer Testing* 57 (2017): 219–225. DOI: 10.1016/j.polymertesting.2016.11.035.
[24] Böhm, H. J. "A Short Introduction to Continuum Micromechanics." *Mechanics of Microstructured Materials*. Ed. Helmut J. Böhm. Vienna: Springer Vienna, 2004. pp. 1–40. DOI: 10.1007/978-3-7091-2776-6_1.
[25] Mori, T., Tanaka, K. "Average stress in matrix and average elastic energy of materials with misfitting inclusions." *Acta Metallurgica* 21 (1973): 571–574. DOI: 10.1016/0001-6160(73)90064-3.

[26] Eshelby, J. D. "The determination of the elastic field of an ellipsoidal inclusion, and related problems." *Proceedings of the Royal Society of London. Series A. Mathematical and Physical Sciences* 241 (1957): 376–396. DOI: 10.1098/rspa.1957.0133.
[27] Christensen, R. M. "A critical evaluation for a class of micro-mechanics models." *Journal of the Mechanics and Physics of Solids* 38 (1990): 379–404. DOI: 10.1016/0022-5096(90)90005-O.
[28] Kaiser, J.-M. *Beitrag zur mikromechanischen Berechnung kurzfaserverstärkter Kunststoffe - Deformation und Versagen*. PhD thesis, Saarbrücken, 2013.
[29] J. C. Halpin, Kardos, J. L. "The Halpin-Tsai equations: A review." *Polymer Engineering and Science* 16 (1976): 344–352. DOI: 10.1002/pen.760160512.
[30] Tandon, G. P., Weng, G. J. "The effect of aspect ratio of inclusions on the elastic properties of unidirectionally aligned composites." *Polymer Composites* 5 (1984): 327–333. DOI: 10.1002/pc.750050413.
[31] Schöneich, M. M. *Charakterisierung und Modellierung viskoelastischer Eigenschaften von kurzglasfaserverstärkten Thermoplasten mit Faser-Matrix Interphase*. PhD thesis, Saarbrücken, 2016. DOI: 10.22028/D291-23208.
[32] Dassault Systèmes. *Abaqus 2018 Theory Guide*, 2017.
[33] Gieß, M. *Untersuchungen zur akustischen Formteilauslegung*. PhD thesis, Aachen: Shaker, 2019.
[34] Barbero, E. J. *Finite element analysis of composite materials using ANSYS*, Boca Raton Fla.: CRC Press, 2nd ed., 2014.
[35] Advani, S. G., Tucker, C. L. "The Use of Tensors to Describe and Predict Fiber Orientation in Short Fiber Composites." *Journal of Rheology* 31 (1987): 751–784. DOI: 10.1122/1.549945.
[36] Abdin, Y. *Micro-mechanics based Fatigue Modelling of Composites Reinforced with Straight and Wavy Short Fibers*. PhD thesis, Leuven, 2015.
[37] Kohnke, P. C. *ANSYS - engineering analysis system theoretical manual for Rev. 4.4*, Houston: Swanson Analysis Systems Inc., 5th ed., 1989.
[38] Urban (né Pfeifer), F., Armbruster, B. "Vorrichtung zur Schwingungsanregung eines Probekörpers." Patent DE 10 2019 001 226.7, 2019, https://register.dpma.de/DPMAregister/pat/register?AKZ=1020190012267.